DICHROIC DESIGN FOR THE ORBITING VLBI EARTH STATION ANTENNA

T. K. Wu and W. P. Shillue

ABSTRACT

In this paper the design and performance of a single screen frequency selective surface (FSS) with gridded square loop patch elements are described for diplexing the X- and Ku- band signals in an orbiting Very Long Baseline Interferometer (OVLBI) earth station reflector antenna system. Excellent agreement is obtained between the predicted and measured results. This validates the FSS design using the gridded square element. As the grid is sandwiched between two 0.035" thick Teflon (or PTFE) slabs, the resonant frequency drift is reduced by 1GHz with the incident angle steered from normal to 40°.

INTRODUCTION

Orbiting Very Long Baseline Interferometer (OVLBI) is a new branch of radio astronomy, involving extension of the VLBI technique to include radio telescopes placed in orbit around the earth. Typically, VLBI involves simultaneous observations from widely separated radio telescopes, followed by correlation of the signals received at each telescope in a central processing facility. VLBI has been an important technique in radio astronomy for over 20 years because it produces images whose angular resolution is far higher than that of any other technique.

Currently, the National Radio Astronomical Observatory (NRAO) is constructing an earth station at Green Bank, West Virginia to communicate with two OVLBI satellites, i.e., the Russian RADIOASTRON and the VLBI Space Observatory Project (VSOP) by Japan, as illustrated in Figure 1. The frequency allocations for the communication between this earth station and the two satellites are in the X- and Ku-bands, as described in Table 1. To meet this dual-band communication requirement, the multi-reflector antenna with a flat panel frequency selective surface (FSS) or dichroic, as shown in Figure 2, has been proposed. In this configuration, the flat FSS should be designed to reflect Ku-band signals (13.5 to 15.5 GHz) and to pass X-band signals (7 to 9 GHz). Because the satellite link is in circular polarization, the FSS must have similar response to left- and right-hand circular polarizations (LHCP and RHCP), and by extension, to transverse electric and transverse magnetic (TE and TM) incidence. In order to reduce the antenna's noise temperature, the RF insertion loss (including the ohmic loss) of the FSS should also be minimized for incident angle range from normal to 40°.

In the past, the cross-dipole patch element FSS was used for the subreflector design in the reflector antennas of Voyager [1] for reflecting the X-band waves and passing the S-band waves, and the Tracking and Data Relay Satellite System (TDRSS) for diplexing the S- and Ku- band waves [2]. The characteristics of the cross-dipole element FSS changes drastically as the incident angle is steered from normal to 40°. Thus a large band separation is required to minimize the RF losses for these dual band applications. This is evidenced by the reflection and transmission band ratio (fI/f,) being 7:1 for single screen FSS [?,] or 4:1 for double screen FSS [1] with cross-dipole patch elements. Better elements arc. definitely needed to achieve smaller frequency-band separations (f_r/f_t = 14.5/8.0 = 1.8) and less sensitivity to the incident angle variation as stated in the above mentioned requirements.

FSSs with gridded square loop patch elements [3], as shown in Figure 3, have been designed for frequency-band ratio (f_r/f_t) from 1.5 to 2. The resonant frequency is fairly stable with respect to changes in the incident angle and polarizations. The grid geometry is symmetrical in the x and y directions. This implies that it is also good for circular polarizations. Therefore, the gridded square loop FSS was selected for this specific application. The FSS design and its performance arc. described in the following sections.

Thin Screen Design Approach

To minimize the ohmic loss, the conducting gridded square loop patches, as shown in Figure 3, were printed on a thin Kapton film (with 0.003" thickness, 3.5 dielectric constant and 0.01 loss tangent). The grid dimensions are given in Table 2. This thin screen FSS can be supported by a fiberglass frame or by a rigid and RF-transparent foam block. The analysis and design of this gridded square loop FSS arc based on the accurate and versatile integral equation technique with subdomain expansion functions described in [4].

The predicted transmission performance of this thin screen gridded square loop FSS is illustrated in Figure 4 as a function of the incident angle and frequency for both TE and TM polarizations. Figures 5 and 6 show the good agreement representatively between the predicted and measured performance at $\Theta_i = 30°$ with TE and TM polarization, respectively. This verifies the gridded square loop FSS's design approach as well as the accuracy of the design software. Table 3 summarizes the computed RF losses of this thin dichroic. The loss at 7, 8 and 9 GHz is the transmission loss, and the loss at 13.5, 14.5 and 15.5 GHz is the reflection loss.

Improved Design Approach

Notice in Figure 4 the resonant frequency shifts about 1.5 GHz as the incident angle is steered from normal to 40°. However, it was found that, by dielectrically loading the thin FSS, one can stabilize the resonant frequency drift due to variations in the incident angle and the field polarization [5-8]. Therefore, this thin screen FSS may further be sandwiched between two low loss teflon (or PTFE) slabs (with 2.2 dielectric constant and 0.005 loss tangent), as illustrated in Figure 3, to reduce the resonant frequency drift (or enlarge the reflection bandwidth). Due to the dielectric loading, the grid dimensions are scaled down as listed in Table 2 for this design. Figure 7 shows the predicted transmission performance when the grid is sandwiched between two 0.035" thick teflon slabs. Figures 8 and 9 show representatively the good agreement between the predicted and measured results at $\Theta_i =$ 30° for TE and TM polarization, respectively. Note the resonant frequency shift for this new design is reduced to less than 1 GHz as the incident angle is steered from normal to 40°.

Tables 5 and 6 summarize the measured 0.5 dB and 20 dB transmission loss bandwidth, respectively, for both the thin and the sandwich FSS. Note that the frequency band with a 20 dB transmission 10ss is the FSS's reflection band because most the incident energy is reflected by the FSS. Typically, th c rc.fleet ion bandwidth increases (or decreases) for the TE (or TM) polarization as the incident wave steered from 0° to 40°. Therefore, the common reflection bandwidth for both TE and 'I'M polarizations is rather mall for the thin screen FSS. However, by sandwiching the thin screen FSS, the common reflection bandwidth increases significantly, as listed in "J'able 6.

conclusion

In this paper the design and performance of a single screen FSS with gridded square. loop patch element arc described for diplexing the X- and Ku-band signals in an OVLBI earth station reflector antenna system. The validity of the FSS designs using the gridded square element is verified by the excellent agreement obtain ccl between the predicted and measured results. in addition, the resonant frequency drift with change of incident angle, is reduced by 1 GHz as the grid is sandwiched between two 0.035" thick Teflon slabs. It is recommended to investigate further the integrated dichroic and reflector antenna's performance by the analytical technique [9] and measurements.

Acknowledgement

The research described in this paper was carried out by Jet Propulsion Lab., California Institute of Technology under contract with NASA. The FSSs and some test results were obtained by NRAO. The authors wish to thank Mr. R. Thomas of J])], for making the measurement, Mr. L. D'Addario of NRAO and Mr. R. Petrie of JPL for their support and encouragement during the course of this task.

References

1. G.H. Schennum, "Frequency selective surfaces for multiple frequency antenn as," Microwave Journal, vol. 16, no.5, pp. 55-57, May 1973.

2. V.D. Agrawal and W.A. Imbriale, "Design of a dichroic Casegrain subreflector," IEEE Trans., vol. AP-27, no.7, pp. 4 66-473, July 1 979.

3. C. K. Lee and R. Langley, "1 Equivalent circuit models for frequency selective surfaces at oblique. angle of incidence, " IEE Proceedings, vol.132, part II, no. 6,])]).395-398, Oct. 1985.

4. R. Mittra, C.H. Chan, and T. Cwik, "Techniques for analyzing frequency selective surface - a review, " Proceedings of the IEEE, vol. 76, 110.1 ?., pp. 1593-1615, Dee, 1988.

S. C.C. Chen, "Diffraction of electromagnetic waves by a conducting screen perforated periodically with circular holes," IEEE Trans., vol. AP-19, no. 3, pp. 475-481, May 1971.

6. B. Munk and T. Kornbau, "On stabilization of the bandwidth of a dichroic surface by use of dielectric slabs," Electromagnetics, vol. 5, no.4, pp. 349-3"/3, 1985.

7. T.K. Wu, "Single-screen triband FSS with double-square-loop elements," Microwave and Optical Technology Letters, vol. 5, no. 2, pp. 56-59, Feb. 1 992.

8. T.K. Wu, "A high Q bandpass structure for the selective transmission and reflection of high frequency radio signals," U.S. Patent no. 5103241, April 1992.

9. T.K. Wu, S.W. Lee and M.L. Zimm erman, "1 Evalu at ion of frequency selective reflector antenna systems," Microwave and Optical Technology I/et t ers, vol. 6, 110.3,])]). 175-179, March 51993.

TABLE 1. Reflector Antenna Requirements

Frequency (GHz)	Bandwidth (GHz)	Usage	Polarization
7.22	0.045	RADIOASTRON Uplink	LHCP
8.47	0.1	RADIOASTRON Downlink	RHCP
14.2	0.1	VSOP Downlink	LHCP
15.3	0.1	VSOP Uplink	LHCP

TABLE 2. The Dimensions (inches) of Gridded Square Loop FSSs

Design	W_1	W_2	P	G
Thin Screen	0.022	0.0443	0.3543	0.022
Improved	0.0167	0.0335	0.2677	0.0167

TABLE 3. Computed Thin Screen FSS Insertion Loss Summary (dB)

Frequency (GHz)	Θ_i = 0°	30° TE	30° TM	40° TE	40° TM
7.0	.56	.84	.58	1.14	.56
8.0	.04	.1	.06	.17	.07
9.0	.2	.17	.15	.16	.11
13.5	.2	.11	.08	.06	.03
14.5	.02	.01	.05	.02	.15
15.5	.06	.14	.35	.19	.68

TABLE 4. Computed Sandwich FSS Insertion Loss Summary (dB)

Frequency (GHz)	Θ_i = 0°	300 TE	300 TM	40° TE	40° TM
7.0	.52	.75	,57	.998	.58
8.0	.0'1	.04	.03	.04	.04
9.0	.77	.87	.51	.998	.35
13.5	.14	.09	.12	,06	.1
14.5	.02	,02	.02	.02	.03
15.5	.05	.08	.14	.09	.25

TABLE 5. Measured 0.5 dB Transmission Loss Bandwidth (GHz)

	Thin Screen FSS		Sandwich FSS	
Angle (deg.)	TE	TM	TE	TM
0	7.2- 8,S	7.2 -8,5	7.2 -8.6	7.2 -8.4
15	7.2 -8.5	7.2- 8.5	7.2 -8.6	7.3 -8.7
30	7.4 -8.9	7,2 -8.7	7.2 -8.4	7.2 -8.4
40	7.6 -8.9	7,3 -9,0	7.?. -8.4	7.1 -8.8
	Common Bandwidth: 7.6 - 8.5		Common Bandwidth: 7.3- 8,4	

TABLE 6. Measured 20 dB Transmission Loss Bandwidth (GHz)

	Thin Screen FSS		Sandwich FSS	
Angle (deg.)	TE	TM	TE	TM
0	13.8 -15.5	13.8 -15.5	13.9 -15.7	14.0 - 15.8
15	13.7 -15.3	13.8 -15.1	14.0 - 15.6	14.0 -15.6
30	13.5 -15.0	13.4 -14.5	13.8 -15.5	13.9-15.?
40	13.4 -14.7	13.1 -14.0	13.7 -15.5	13.9 -15.1
	Common Bandwidth: 13.8 -14.0		Common Bandwidth: 14.0 -15.1	

Figure Titles

1. Scenario of orbiting very long baseline interferometry (OVLBI).

2. OVLBI earth station reflector antenna configuration (drawing, not to scale).

3. Gridded square loop element FSS design configurations.

4. Predicted transmission performance of the thin semen FSS.

5. Comparison of the measured and computed transmission performance. of the thin FSS, 30° TE incidence.

6. Comparison of the measured and computed transmission performance of the thin FSS, 30° TM incidence.

7. Predicted transmission] performance of the sandwich FSS.

8. Comparison of the measured and computed transmission performance of the sandwich FSS, 30° TE incidence.

9. Comparison of the measured and computed transmission performance of the sandwich FSS, 30° TM incidence.

Figure 1. Scenario of Orbiting Very Baseline Interferometry (OVLBI).

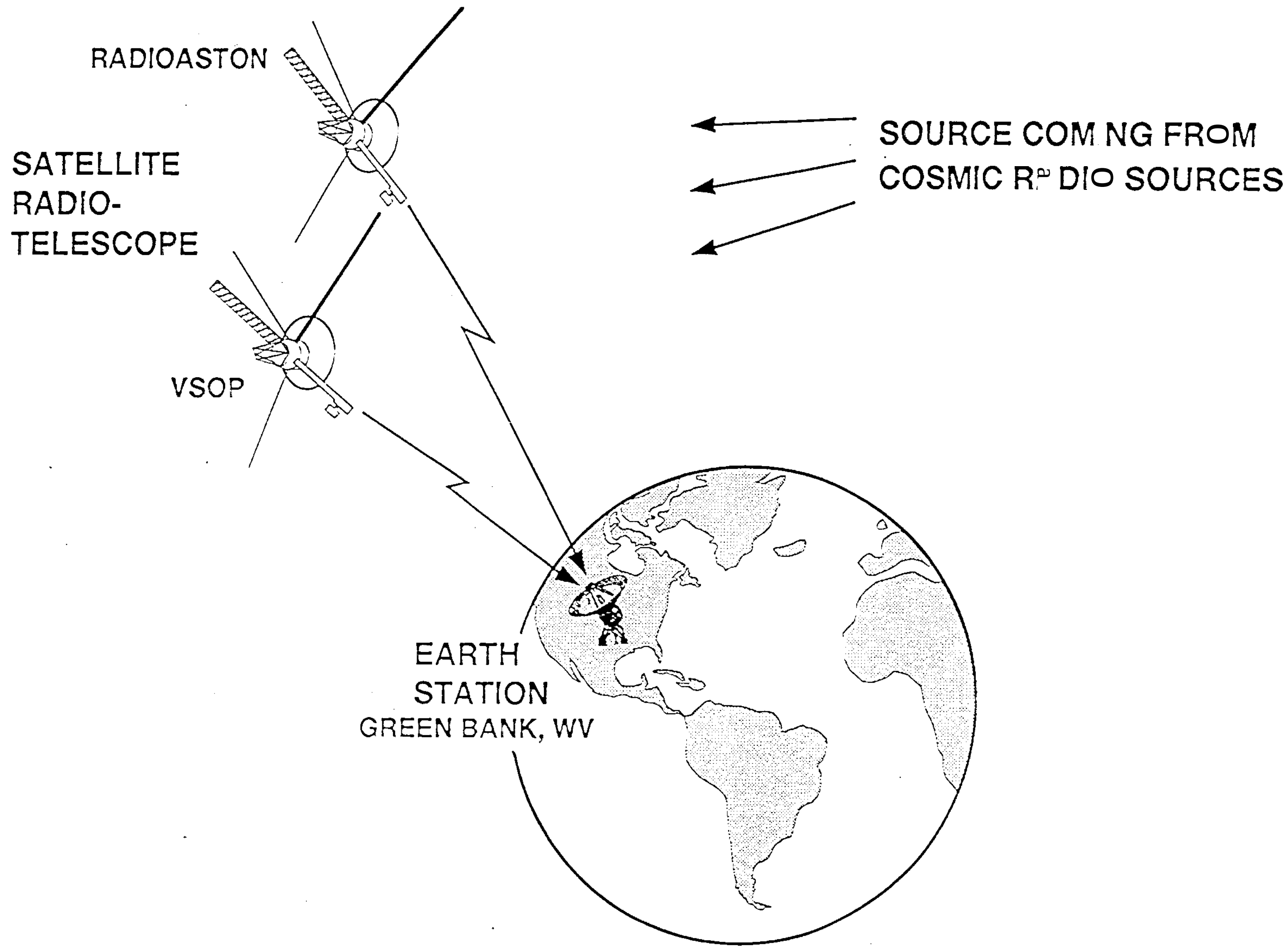

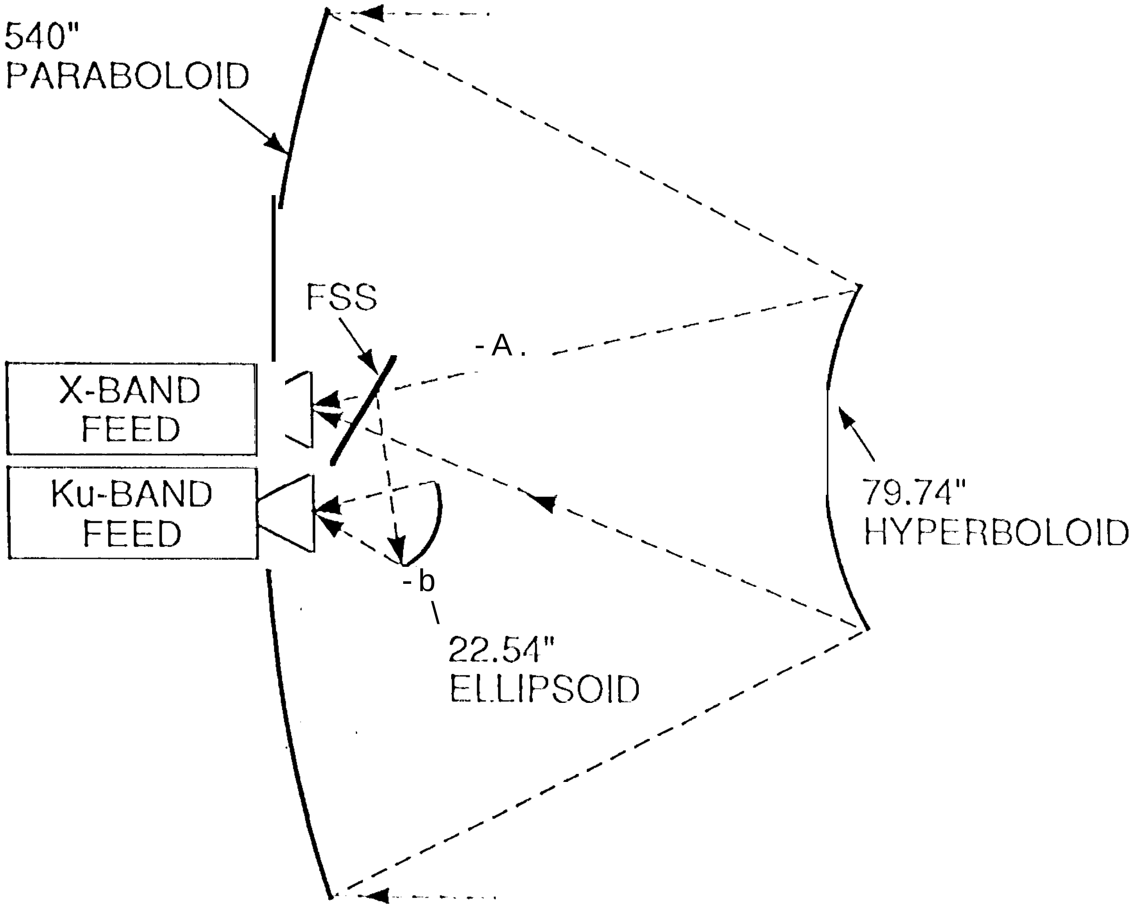

Figure 2. OVLBI Earth Station Reflector Antenna Configuration

(drawing not to scale).

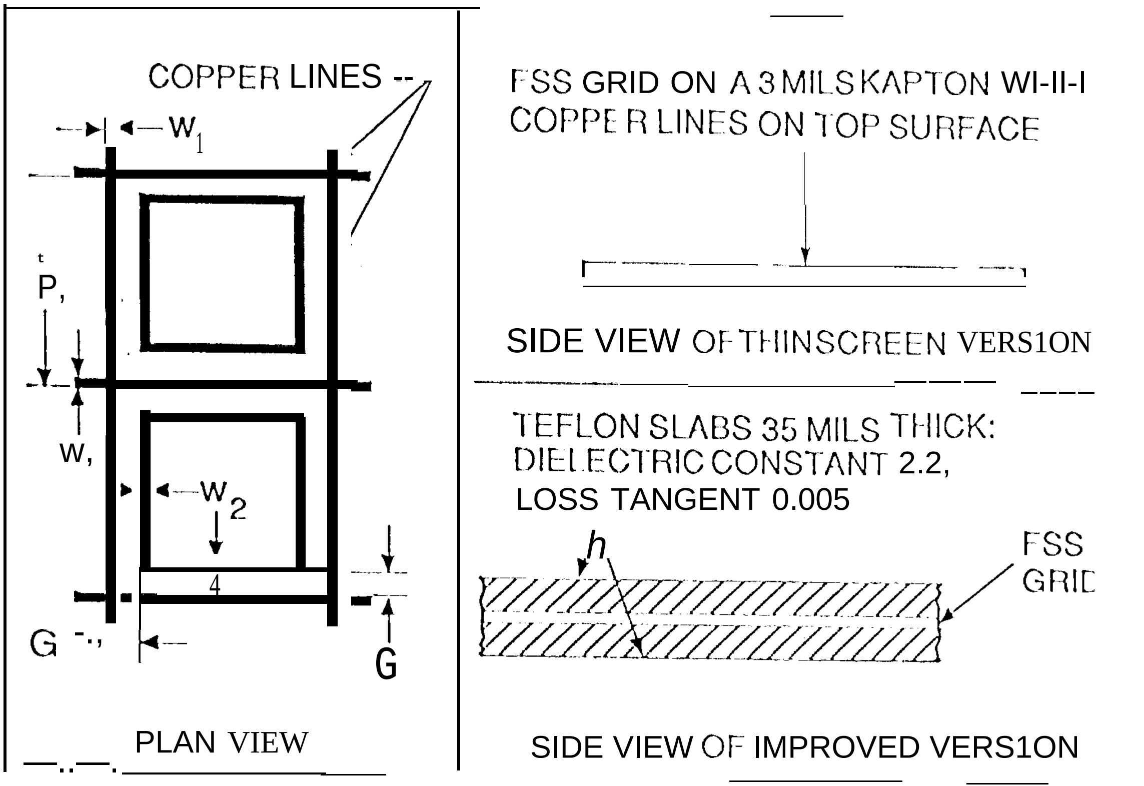

Figure 3. Gri dded Square Loop Element FSS Design Configurat ions

Figure 4. Predicted Transmission Performance of the Thin Screen 1“ss

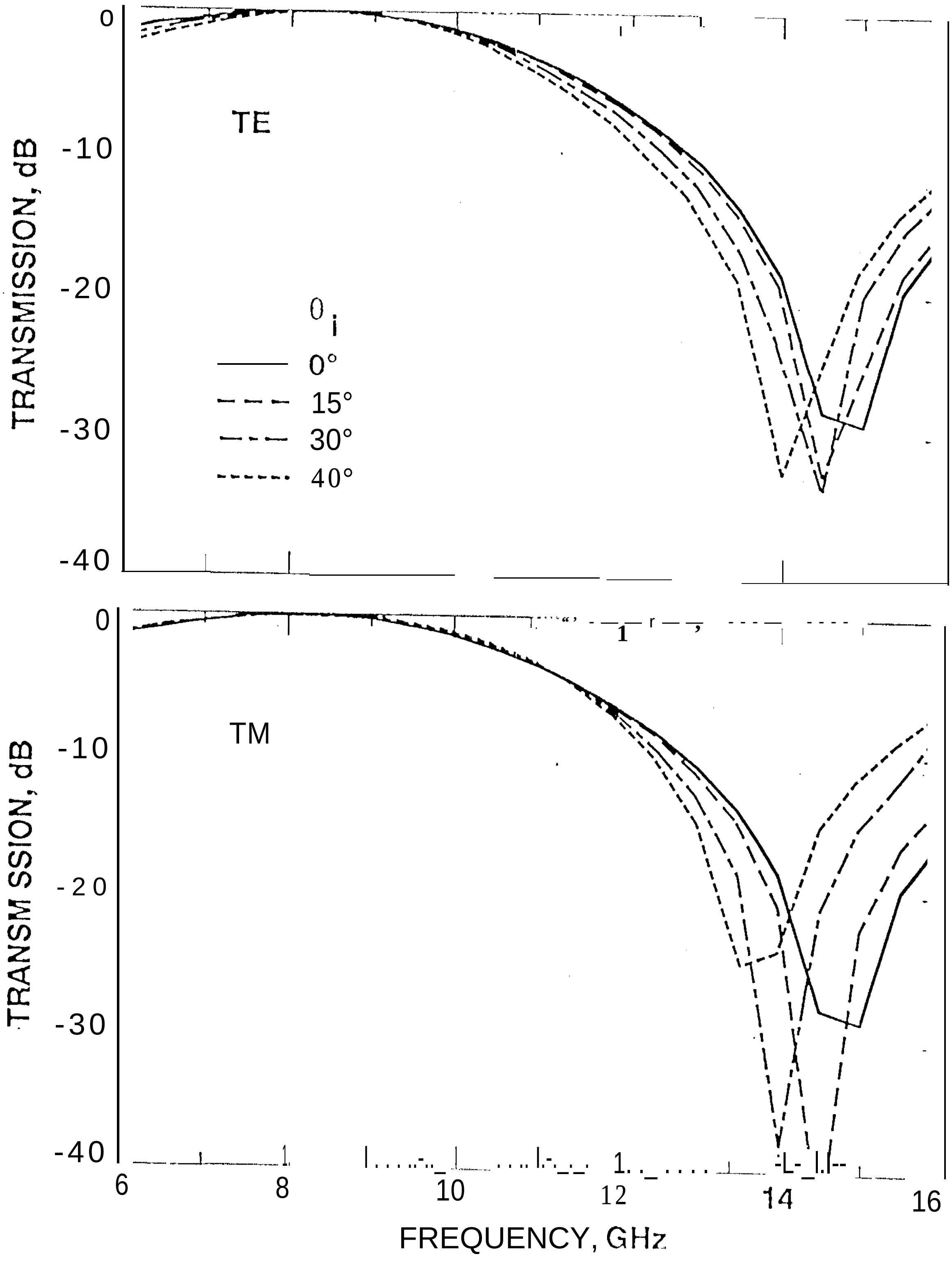

Figure 5. Comparison of the measured and computed transmission performance of the thin FSS, 30° TE incidence.

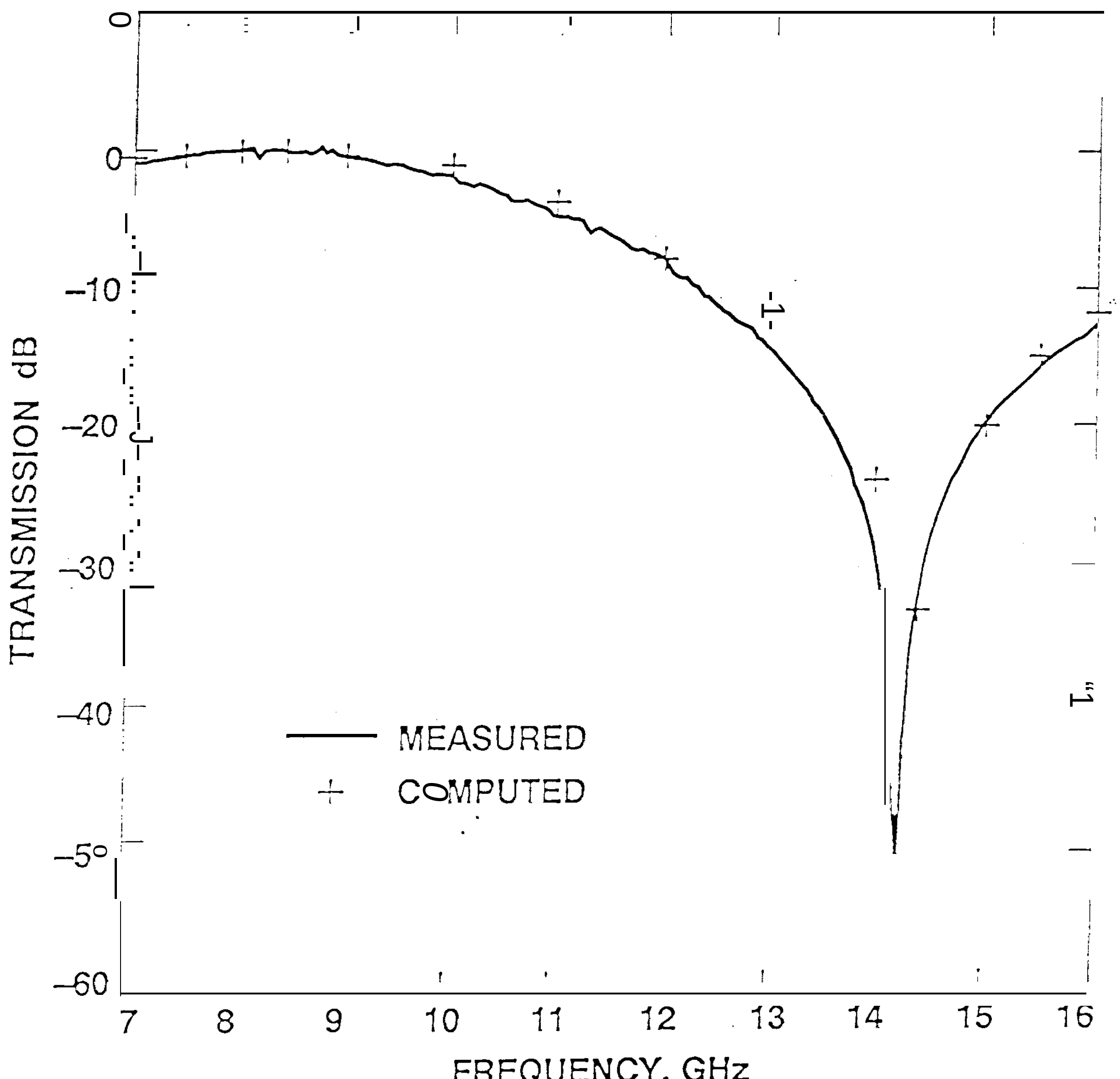

Figure 6. Comparison of the measured and computed transmission performance of the thin FSS, 30° TM incidence.

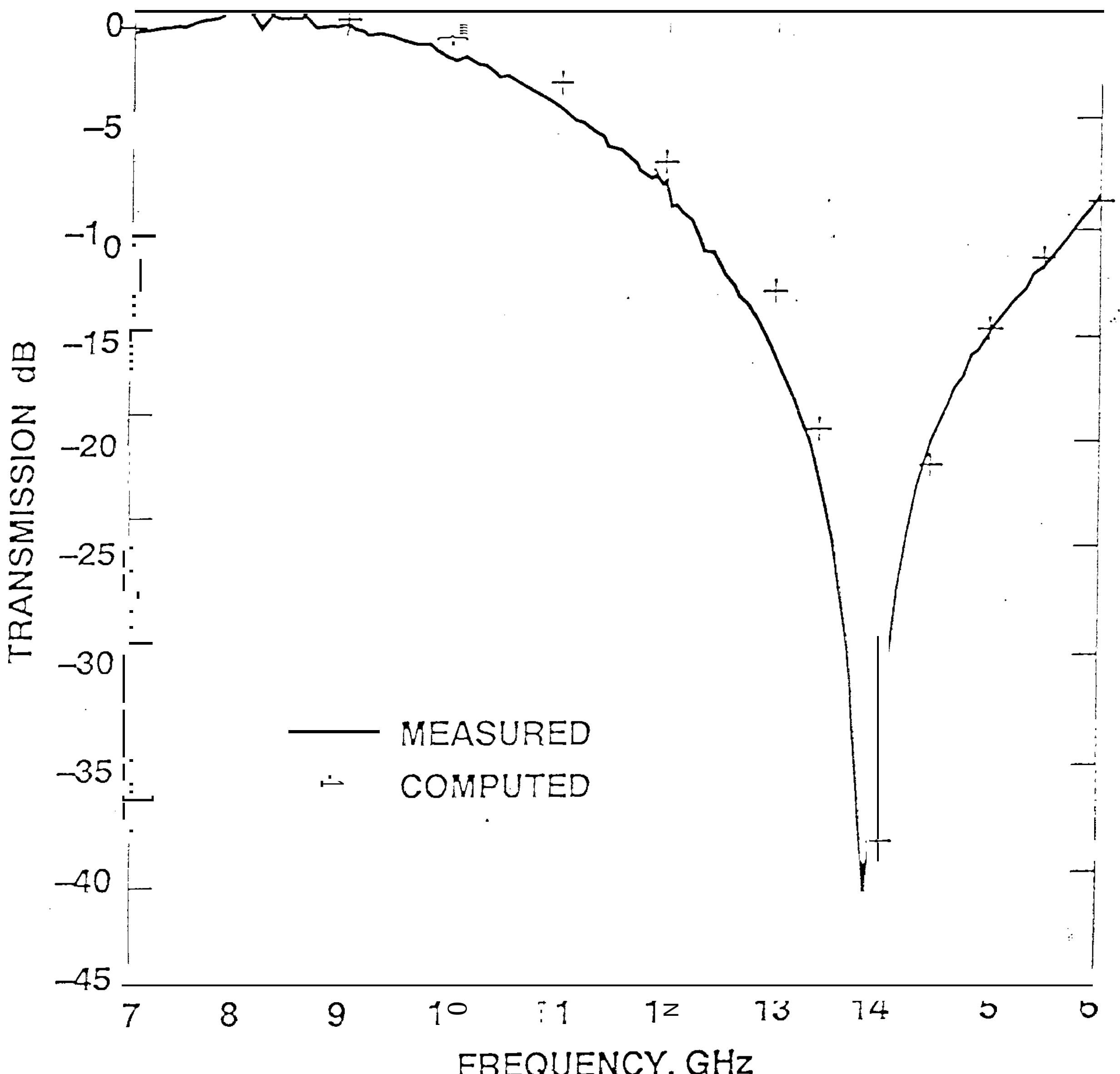

Figure 7. Predicted transmission performance of the sandwich FSS.

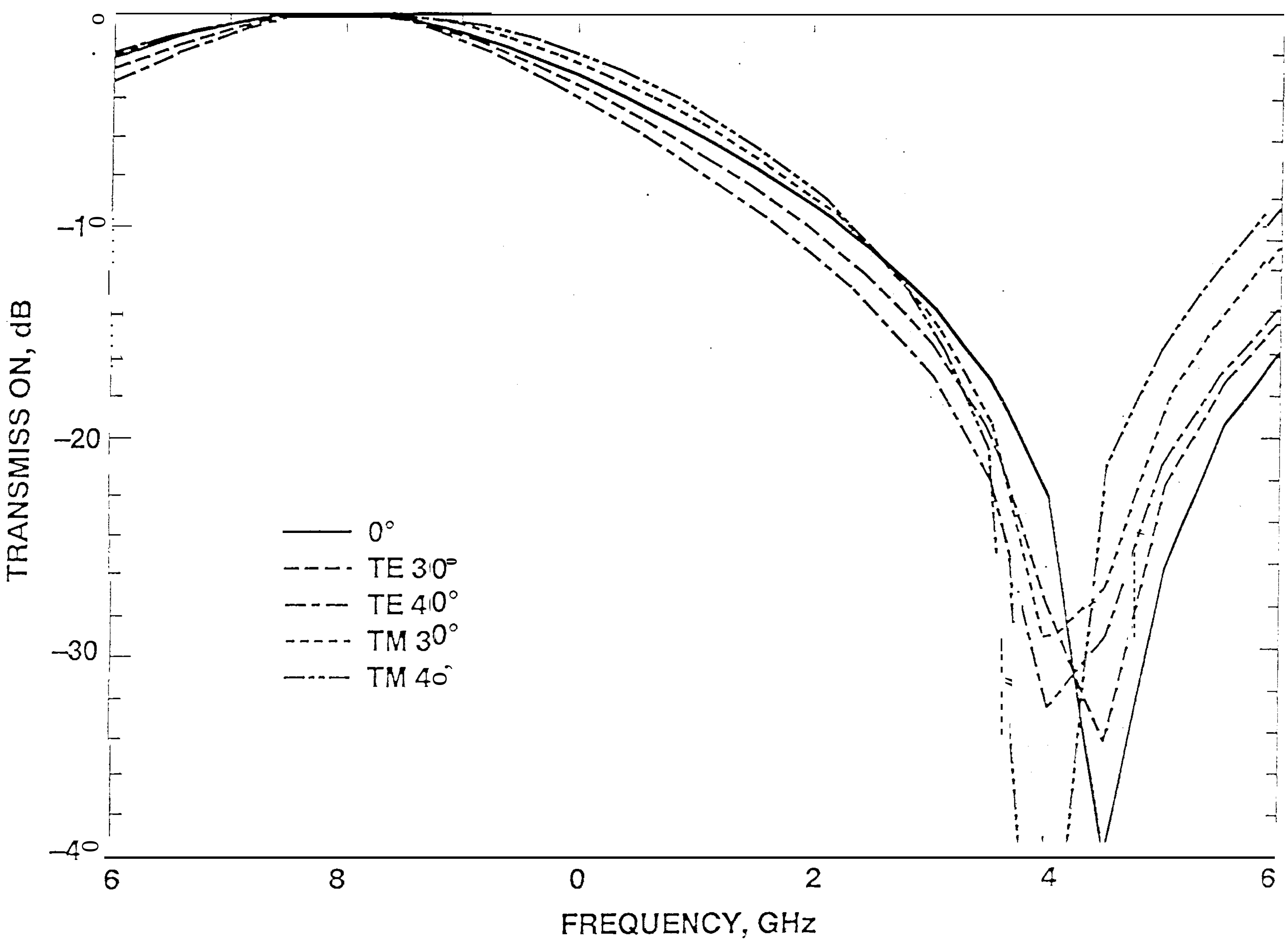

Figure 8. Comparison of the measured and computed transmission performance of the sandwich FSS, 30° TE incidence.

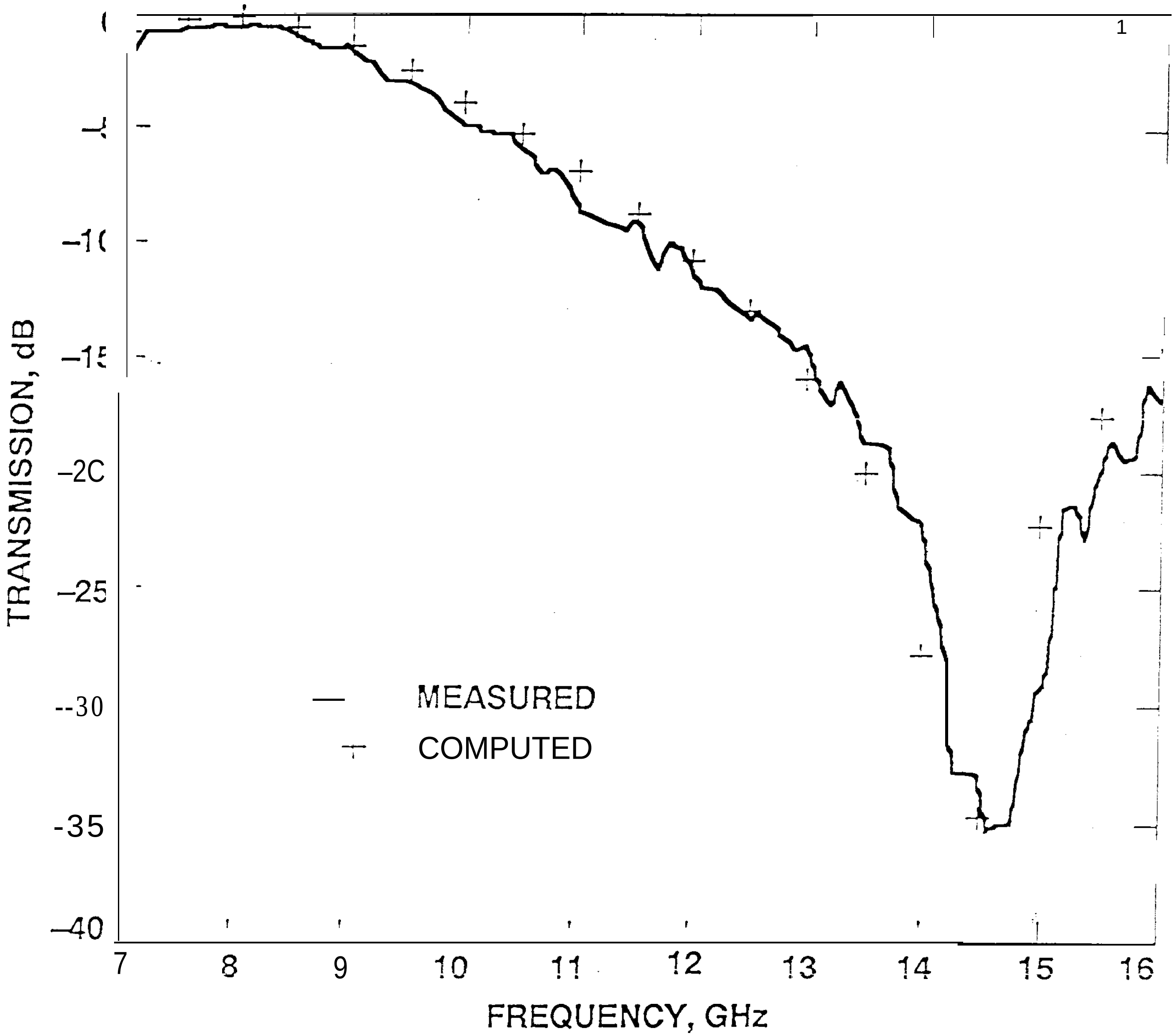

Figure 9. Comparison of the measured and computed transmission performance of the sandwich FSS, 30° TM incidence.